Ligand Exchange Dynamics in Aqueous Solution Studied with 2DIR Spectroscopy

Sungnam Park,[†,‡] Minbiao Ji,[†,§] and Kelly J. Gaffney*[,†]

PULSE Institute for Ultrafast Energy Science, SLAC National Accelerator Laboratory, Stanford University, Stanford, California 94305, Department of Chemistry, Korea University, Seoul, 136-701, Republic of Korea, and Department of Physics, Stanford University, Stanford, California 94305

We have used time-resolved multidimensional vibrational spectroscopy, generally termed 2DIR spectroscopy, to study the equilibrium dynamics of ligand exchange in an aqueous solution containing 3.4 M $Mg(ClO_4)_2$ and 1.2 M NaSCN. The sensitivity of the CN stretching frequency of thiocyanate (SCN^-) to contact ion pair formation with Mg^{2+} ions generates distinct spectroscopic signatures for the $MgNCS^+$ contact ion pair and the free SCN^-. We have utilized 2DIR spectroscopy to successfully resolve the interconversion between these thiocyanate configurations and measured the $MgNCS^+$ contact ion pair dissociation time constant to be 52 ± 10 ps. We attribute the observed dynamics to perchlorate−thiocyanate anion exchange in the first solvation shell of the Mg^{2+} cation. Magnesium ions in this concentrated ionic solution will be coordinated by water molecules, as well as perchlorate and thiocyanate ions. While prior studies have observed microsecond residence times for water ligands in the first coordination sphere of Mg^{2+}, our study represents the first experimental observation of anion exchange in the first solvent shell of the Mg^{2+} cation. We have also used orientational relaxation and spectral diffusion dynamics to quantify the dynamical distinctions between the free anion and the anion in the contact ion pair.

I. Introduction

The variable reactivity of a chemical substrate in the presence or absence of a solvent, a heterogeneous catalyst, or an enzymatic protein highlights the significant impact the reaction environment has on chemical dynamics. While the influence of reaction environment has been extensively investigated for photochemical reactions, dynamical studies of equilibrium chemical dynamics remains a novel area of investigation[1−4] with significant opportunity to complement and enhance molecular dynamics simulations of equilibrium chemical dynamics.[5−8]

Ligand exchange in solution represents a fundamental solvent-controlled reaction.[7,9] While the separation between ligand and metal ion provides the intuitive reaction coordinate,[5,6,10] fluctuations in the solvent structure surrounding the ligand−metal ion pair explicitly influence the solution phase reaction mechanism.[7] Molecular dynamics (MD) simulations provide the most direct route to mechanistic understanding of thermal reaction dynamics in ionic solutions, but the 20 to 30 ps durations of ab initio molecular dynamics simulations[11−16] limit the accessible conformational dynamics and classical simulations depend upon the empirical force fields utilized to perform the MD simulations.[5−10,17] Given these limitations, benchmark dynamical measurements provide a critical complement to the MD simulation studies.

A variety of spectroscopic methods have been utilized to study the equilibrium and dynamical properties of ionic solutions.[18−32] Dielectric and ultrasonic relaxation spectroscopy have proven particularly useful for studying the dynamic properties of ionic solutions, providing information about the association and rotation of contact ion pairs (CIP), solvent separated ion pairs

(SIP), and doubly solvent separated ion pairs (2SIP).[21,23,29−31] This sensitivity also makes analysis challenging, since the contribution of each ion pair configuration to the spectrum overlap and the dynamics of ion pair rotation and dissociation can be difficult to distinguish. This has proven to be particularly true for ion pairing in aqueous solutions,[33] where the rate of ion pair dissociation has generally been observed for strongly associating ion pairs.[21,29,34] These measurements have observed ion pair dissociation on the nanosecond to microsecond time scale and have been generally insensitive to the picosecond time scale dynamics accessible to molecular dynamics simulations.[5−8]

Time-resolved IR spectroscopy of molecular anions provides an alternative approach to characterizing ionic equilibria and dynamics in solution. The IR spectra of a variety of anions shift measurably when they form a CIP with alkali and alkaline earth metal cations in polar solvents,[35−39] but the spectra do not distinguish among SIP, 2SIP, and free anions. Of these molecular anions, thiocyanate (SCN^-), isocyanate (OCN^-), and azide (N_3^-) provide the most tractable IR spectroscopy, particularly for time-resolved measurements.[32,39,40] Due to the longer excited state lifetime of the antisymmetric CN stretch of SCN^-,[40,41] we have used this anion to study ion pairing in water. For aqueous solutions of Mg^{2+} and SCN^-, the $MgNCS^+$ contact ion pair (CIP) has a CN stretch frequency of 2110 cm^{-1}, while all other SCN^- ionic configurations lead to absorption at 2068 cm^{-1}. Prior studies of concentrated aqueous $MgSO_4$ solutions indicate that the concentration of free ionic species will greatly exceed the SIP and 2SIP concentrations in the solution we have investigated.[33] The dominance of free ions does not reflect the mean distance between ions, since the majority of ions will be within two solvation shells of a counterion, but rather indicates the ions move independently. These distinct vibrational transition energies for the CIP and the free anion configurations provide the opportunity to use

* To whom correspondence should be addressed. E-mail: kgaffney@slac.stanford.edu.
† PULSE Institute for Ultrafast Energy Science, SLAC National Accelerator Laboratory, Stanford University.
‡ Department of Chemistry, Korea University.
§ Department of Physics, Stanford University.

2DIR spectroscopy to investigate the equilibrium dynamics of ion association and dissociation in aqueous ionic solutions.

Multidimensional vibrational correlation spectroscopy, or two-dimensional infrared (2DIR) spectroscopy, provides a robust experimental method for investigating equilibrium structural and conformational dynamics on the picosecond time scale.[42,43] It has been used to study solute−solvent complexation,[2] C−C single bond rotation,[4] fast protein conformational change,[44] and water's hydrogen bond exchange in aqueous ionic solutions,[45,46] and other hydrogen bond exchange dynamics.[1,3] We have used a solution of 3.4 M $Mg(ClO_4)_2$ and 1.2 M NaSCN dissolved in D_2O to investigate Mg^{2+} and SCN^- association and dissociation dynamics with 2DIR spectroscopy. We have successfully resolved the interconversion between the $MgNCS^+$ CIP and free SCN^- anion configurations. We observe the CIP dissociation time constant to be 52 ± 10 ps. The microsecond dissociation rate for H_2O-Mg^{2+} extracted from NMR and ultrasonic relaxation measurements greatly exceed our CIP dissociation time constant.[23,24,34,47−51] While these frequency domain observations have not been replicated with time domain measurements, the 7.4 kcal/mol activation energy extracted from first-principles MD simulations[16] resembles the 9.5 kcal/mol activation energy measured with NMR.[50] Unless the presence of SCN^- and ClO_4^- ligands greatly modifies the binding energy of water to Mg^{2+},[12,15] the exchange process being observed experimentally seems unlikely to be the interchange of water and SCN^- in the first solvation shell of Mg^{2+}. We associate the picosecond dissociation with perchlorate−thiocyanate anion exchange. For the roughly 7 M perchlorate solution we have investigated, Mg^{2+} ions will have an appreciable concentration of perchlorate and thiocyanate anions in their first solvation shell as supported by IR and Raman spectroscopy.[36]

To gain a more exhaustive understanding of the structural and chemical dynamics in this aqueous ionic solution, we have measured the orientational relaxation and spectral diffusion dynamics of thiocyanate in the free and CIP configurations with polarization-selective IR pump−probe spectroscopy and 2DIR spectroscopy. The impact of CIP formation on the rotational freedom of the thiocyanate anion has been quantified by independently measuring the orientational relaxational dynamics of free SCN^- and SCN^- in the $MgNCS^+$ CIP configuration. Spectral diffusion dynamics provide further insight into the energetics and dynamics of the solute−solvent interaction and how CIP formation modifies these dynamics. Spectral diffusion dynamics have been measured with a variety of time-resolved IR spectroscopic methods, including IR hole-burning experiments,[52−54] three pulse echo peak shift (3PEPS) measurements,[55−57] and line shape analysis of 2DIR spectra.[58−62] For IR spectra with multiple coupled vibrational transitions, Fourier-transform based 2DIR spectroscopy provides the optimal method since spectral and temporal resolution can be varied independently, unlike time-resolved hole-burning experiments, and 2DIR spectroscopy resolves distinct quantum pathways with the same echo frequency, unlike 3PEPS. These measurements of orientational relaxation and spectral diffusion dynamics, in conjunction with 2DIR spectroscopic measurement of chemical exchange dynamics, provide a detailed characterization of ion dynamics in the aqueous ionic solution we have investigated.

II. Experimental Section

The laser system employed in the experiments was built based on a design that has been described in detail elsewhere.[63] Briefly, 800 nm pulses were generated by a Ti:Sapphire oscillator (KM Laser) and regenerative amplifier (Spitfire, Spectra-Physics) laser

system at 1 kHz. The 800 nm pulses with 45 fs duration and ∼0.8 mJ per pulse were used to pump an optical parametric amplifier (OPA, Spectra-Physics) to produce near-IR pulses at ∼1.4 and ∼1.9 μm which were utilized to generate mid-IR pulses at 2050 cm^{-1} in a 0.5 mm thick $AgGaS_2$ crystal by difference frequency generation (DFG). The power spectrum of the mid-IR pulses had a Gaussian envelope with a ∼270 cm^{-1} bandwidth (full width at half-maximum). After generation, the mid-IR pulses propagate through an experimental setup purged with dry and CO_2 scrubbed air. We measured the pulse chirp with frequency-resolved optical gating (FROG) measurements in a transient grating geometry.[63] We used CaF_2 plates with different thicknesses to compensate for the linear dispersion introduced by other dielectric materials in the setup, particularly a Ge Brewster plate. This setup produced transform-limited mid-IR pulses with pulse duration of ∼55 fs at the sample.

The experimental details and principles of multidimensional vibrational correlation spectroscopy, generally termed two-dimensional infrared (2DIR) spectroscopy, have been described in detail elsewhere.[60,61,63,64] We focus three mid-IR pulses with an off-axis parabolic mirror (f.l. = 150 cm) onto the sample in a noncollinear geometry and collimate the beams after the sample with another off-axis parabolic mirror (f.l. = 150 cm). The spot size of the IR beams at the sample position is approximately 100 μm in diameter. We control the relative time of these three pulses with computer-controlled translational stages. The sample emits the signal in a unique phase-matched direction, which we overlap with a local oscillator pulse for heterodyne detection. A grating in a spectrometer disperses the heterodyned signal onto the top stripe of a dual 32 × 2 element mercury−cadmium−telluride (MCT) array detector with high-speed data acquisition electronics (Infrared Associates and Infrared Systems Development Corp.). A portion of the IR beam that does not go through the sample is sent to the bottom stripe of the array and used as a reference beam. In 2DIR experiments, there are three experimental time variables. The delay between the first and second pulses corresponds to the evolution time (τ), the delay between the second and third pulses corresponds to the waiting time (T_w), and the delay between the third pulse and the emitted signal corresponds to the detection time (t). We measure the 2DIR signal by scanning τ at fixed T_w and frequency-resolving the heterodyned signal onto the pixel array detector. To construct the 2DIR spectra, we must Fourier transform the τ and the t time periods. The spectrometer performs the detection time (t) Fourier transform to generate the ω_m axis, while we numerically Fourier transform the τ time period after collecting the τ-dependent interferogram for each value of ω_m. This Fourier transformation provides the ω_τ axis. 2DIR spectra are displayed with initial frequency ω_τ and final frequency ω_m at a fixed T_w time. We generate purely absorptive 2DIR spectra with the dual scan method, in which nonrephasing and rephasing 2DIR spectra are measured separately by two different input pulse sequences and added.[65]

In IR pump−probe experiments, an IR pump pulse excites a molecular system to the first vibrational excited state ($v = 1$), and subsequently the time evolution of the molecular system is measured by a time-delayed IR probe pulse. The details of the IR pump−probe experiments have been described elsewhere.[61,66] Mid-IR pulses are split into the pump and probe beams with a relative intensity of 9:1 and are focused onto the sample. The probe beam is collimated after the sample and is dispersed through a spectrometer onto the MCT array detector. The wiregrid polarizers are placed in the pump and probe beam before the sample and in front of the spectrometer. The parallel,
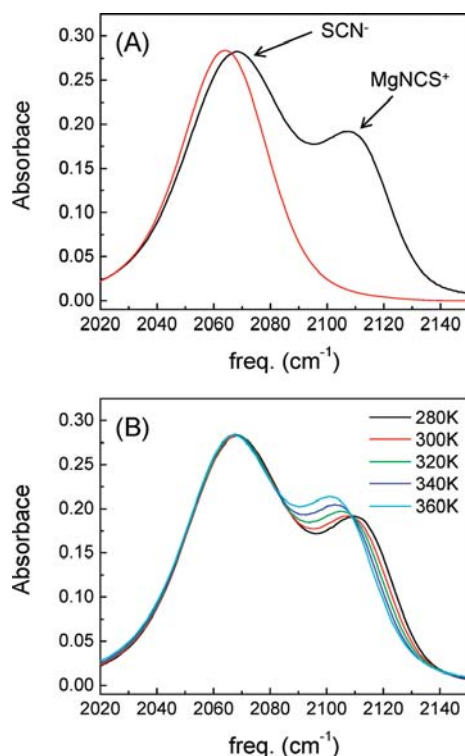
Ligand Exchange Dynamics in Aqueous Solution

J. Phys. Chem. B, Vol. 114, No. 19, 2010 **6695**

Figure 1. FTIR spectra of thiocyanate (SCN⁻) ion in D_2O. (A) NaSCN dissolved in D_2O (red curve), and $Mg(ClO_4)_2$ and NaSCN dissolved in D_2O (black curve). The low-frequency peaks result from free SCN⁻ absorption. The high-frequency peak results from MgNCS⁺ contact ion pair absorption. (B) Temperature-dependent FTIR spectra of $Mg(ClO_4)_2$ and NaSCN dissolved in D_2O. The temperature is increased from 240 to 360 K in 20 deg intervals.

$S_{||}(t)$, and perpendicular, $S_{\perp}(t)$, components of the pump−probe signals at each frequency are measured with the polarization of the pump beam parallel and perpendicular to the probe beam, respectively.

NaSCN, $Mg(ClO_4)_2$, and D_2O were purchased from Sigma-Aldrich and were used as received. NaSCN (0.555 g) and $Mg(ClO_4)_2$ (4.203 g) salts were directly dissolved in 5 g of D_2O ($d = 1.1$ g/mL), preparing an aqueous solution with 1.2 M NaSCN and 3.4 M $Mg(ClO_4)_2$ and a Mg^{2+}:SCN⁻ ratio of 2.75. The sample solution was housed in cells containing two CaF_2 windows (3 mm thick) and a 6 μm thick Teflon spacer to reduce the D_2O background absorption. 2DIR and IR pump−probe experiments were conducted at 22 °C. Temperature-dependent

FTIR experiments were performed by increasing the temperature from 280 to 360 K in 20 deg intervals.

III. Results

A. FTIR Spectroscopy. The linear triatomic thiocyanate anion (SCN⁻) has three IR-active vibrations: the ν_1 symmetric CS stretching mode (747 cm⁻¹), the ν_3 antisymmetric CN stretching mode (2068 cm⁻¹), and the doubly degenerate ν_2 bending mode (470 cm⁻¹) in water.[35] Figure 1A displays the FTIR spectra of a deuterated aqueous solution with 1.2 M NaSCN and 3.4 M $Mg(ClO_4)_2$, as well as a deuterated aqueous solution with 0.5 M NaSCN for comparison. When dissolved in water, NaSCN does not form contact ion pairs and has a single IR absorption at 2064 cm⁻¹ in the frequency range of the ν_3 vibration. Aqueous solutions containing SCN⁻ and Mg^{2+} form *N*-bound 1:1 contact ion pairs (CIP).[36] This leads to two IR absorptions at 2068 and 2110 cm⁻¹ in the frequency range of the ν_3 vibration, as shown in Figure 1A. The MgNCS⁺ CIP absorbs at 2110 cm⁻¹ while the peak at 2068 cm⁻¹ results from the free SCN⁻ anions, solvent separated ion pairs (SIP), and doubly solvent separated ion pairs (2SIP). As discussed in the Introduction, the free SCN⁻ ions should dominate for our concentrated aqueous solution. For simplicity, we will assign the low-frequency peak to free SCN⁻ anions, though a small concentration of SIP and 2SIP should exist as well. Figure 1B displays temperature-dependent FTIR spectra for the sample. As the temperature increases, the high-frequency peak shifts linearly to lower frequency while the low-frequency peak shifts negligibly. This indicates that the strength of the average electrostatic interaction between SCN⁻ and Mg^{2+} ions gradually decreases with increasing temperature due to the increase in the interionic distance. The temperature-dependent modification of the anion−cation and the anion−water interaction also leads to temperature-dependent absorption cross sections. It should be noted that in general, the relative frequency shift ($\Delta\omega$) of the CN stretching vibration in the contact ion pair with respect to that of the free SCN⁻ anion depends upon the strength of the electrostatic interaction between the SCN⁻ and Mg^{2+} ions.[38] In alkali salt solutions (LiSCN, NaSCN, and KSCN), the frequency of the CN stretching vibration in contact ion pairs was found to increase as the charge density of the countercation increased ($\Delta\omega_{K^+} < \Delta\omega_{Na^+} < \Delta\omega_{Li^+}$).[67]

B. 2DIR Spectroscopy. 2DIR spectroscopy monitors thermal equilibrium dynamics occurring on the picosecond time scale by vibrationally labeling molecules with their initial frequencies (ω_τ) and then recording the final frequencies (ω_m) of the initially
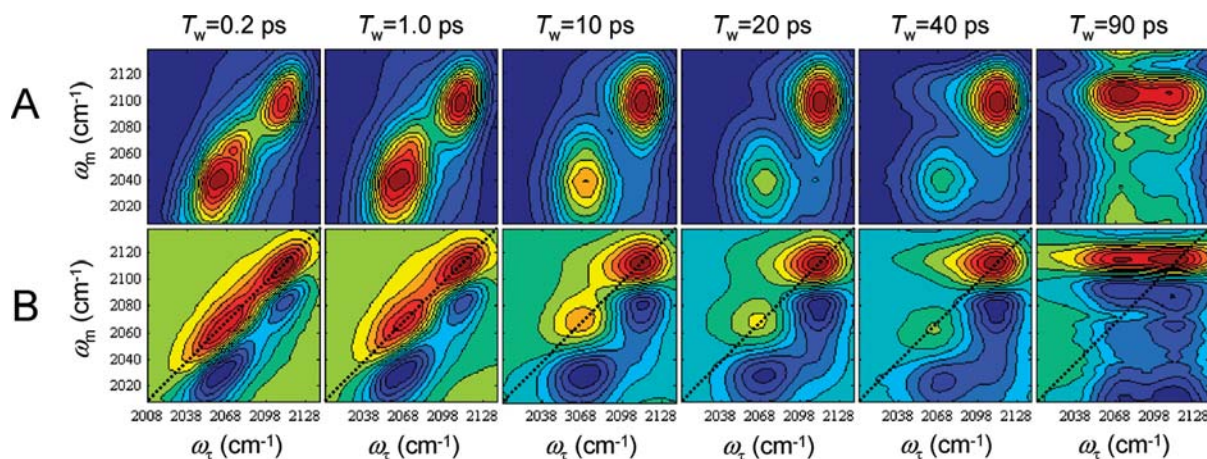

Figure 2. 2DIR spectra obtained from $Mg(ClO_4)_2$ and NaSCN dissolved in D_2O at a series of T_w times with 7% contour lines: (A) amplitude and (B) absorptive spectra. It is clear that the cross peaks grow in as T_w increases.
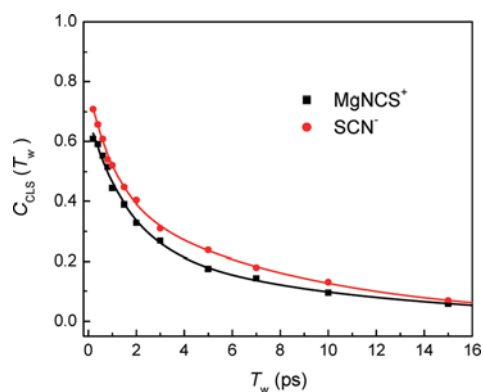
Figure 3. Comparison of spectral diffusion dynamics of free SCN⁻ ion and MgNCS⁺ contact ion pair in D₂O. The experimental inverse of the center line slopes, $C_{CLS}(T_w)$, extracted from the T_w-dependent 2DIR spectra appear as data points and the biexponential fit to the data appears as a solid line.

TABLE 1: Biexponential Fit to the $C_{CLS}(T_w)$

	a_1	τ_1 (ps)	a_2	τ_2 (ps)
free SCN⁻	0.354 ± 0.03	1.11 ± 0.15	0.425 ± 0.03	8.25 ± 0.70
MgNCS+	0.417 ± 0.07	1.64 ± 0.35	0.263 ± 0.08	9.95 ± 1.56

labeled molecules after an experimentally controlled waiting time (T_w).[1–3,45,60,61,63,68] This spectroscopic technique can observe chemical exchange events as slow as a few times the vibrational lifetime and as fast as $1/\Delta\omega$, where $\Delta\omega$ equals the vibrational frequency difference between the interconverting species. 2DIR spectra, $S(\omega_\tau, \omega_m, T_w)$, are displayed by correlating the initial frequency (ω_τ) and final frequency (ω_m) as a function of waiting times (T_w). Figure 2 shows 2DIR spectra obtained at a series of T_w times. Figure 2A shows the amplitudes of the 2DIR spectra and Figure 2B shows the absorptive 2DIR spectra. Both spectra clearly show cross-peak intensity growth with increasing T_w. Figure 2A confirms that the cross-peak intensity does result from chemical exchange and cannot be attributed to a spectral phasing artifact. In Figure 2B, the positive peaks shown in red along the diagonal ($\omega_\tau = \omega_m$) result from the fundamental vibrational transition ($v = 0\rightarrow1$). The high-frequency diagonal peak at $\omega_\tau = \omega_m = 2110$ cm⁻¹ results from the SCN⁻ ions in MgNCS⁺ contact ion pairs while the low-frequency diagonal peak at $\omega_\tau = \omega_m = 2068$ cm⁻¹ comes from the free SCN⁻ ions. The negative peaks appearing in blue color below the diagonal arise from the $v = 1\rightarrow2$ transition, with the value of ω_m red-shifted relative to ω_τ by the vibrational anharmonicity. The 2DIR spectrum at $T_w = 90$ ps results almost entirely from thermally induced changes in the vibrational spectrum, as shown in Figure 1B. This will be discussed in Section III.C.

The T_w-dependent 2DIR spectra reflect a variety of dynamical processes. As T_w increases, vibrational population relaxation and orientational relaxation cause the peak amplitude to decay, spectral diffusion results in a change in the peak shapes, and population exchange between subensembles leads to growth in the cross-peak amplitudes. As seen in Figure 2B, the peak separation of the two peaks resembles the vibrational anharmonicities. This leads to significant overlap in the free anion $v = 0\rightarrow1$ absorption and the free anion to CIP $v = 1\rightarrow2$ cross-

peak absorption, as well as the CIP $v = 1\rightarrow2$ absorption and the CIP to free anion $v = 0\rightarrow1$ cross-peak absorption. However, at $T_w = 40$ ps, the positive cross peak at the upper left corner ($\omega_\tau = 2068$ cm⁻¹, $\omega_m = 2110$ cm⁻¹) and the negative cross peak at the lower right corner ($\omega_\tau = 2110$ cm⁻¹, $\omega_m = 2032$ cm⁻¹) are very clearly observed. The positive cross peak results from the association while the negative cross peak arises from the dissociation. The T_w-dependent cross-peak amplitude in the 2DIR spectra provides the spectroscopic signature of ion association and dissociation dynamics occurring during the T_w time window.

We have also used T_w-dependent peak shape changes in 2DIR spectra to measure spectral diffusion dynamics. Inhomogeneous broadening produces diagonally elongated peaks for small values of T_w. The loss of spectral memory, or spectral diffusion, transforms the diagonally elongated peak into a spectrally symmetric peak as a function of T_w. Therefore, the spectral diffusion dynamics can be quantified by analyzing how the peak shape changes with increasing T_w. Here, we use the center line slope (CLS) method in which the center lines are taken in the T_w-dependent 2DIR spectra and their slopes are inversely proportional to the normalized frequency–frequency correlation function (FFCF), $C(t) = \langle\delta\omega(0)\delta\omega(t)\rangle/\langle\delta\omega(0)\delta\omega(0)\rangle$.[59–62] Figure 3 shows the inverse of the center line slopes, $C_{CLS}(T_w)$, for the free SCN⁻ ion and the MgNCS⁺ CIP. The quality of the data beyond 15 ps does not allow accurate measurements of the inverse of the center line slopes. The $C_{CLS}(T_w)$ is fit with a biexponential function,

$$C_{CLS}(T_w) = a_1 \exp(-T_w/\tau_1) + a_2 \exp(-T_w/\tau_2) \quad (1)$$

The fit parameters can be found in Table 1. The fit results indicate that the $C_{CLS}(T_w)$ for the MgNCS⁺ CIP decays slightly more slowly than that for the free SCN⁻ ion. The detailed analysis will be presented in Section III.C.

C. IR Pump−Probe Spectroscopy. We measured the vibrational population relaxation and orientational relaxation of the free SCN⁻ ion and the SCN⁻ ion in the MgNCS⁺ contact ion pair with polarization-selective IR pump−probe spectroscopy. As mentioned in the previous section, the $v = 0\rightarrow1$ transition (2068 cm⁻¹) of the CN stretching vibration of the free SCN⁻ ion significantly overlaps the $v = 1\rightarrow2$ transition of the CN stretching vibration of the MgNCS⁺ CIP. Therefore, we measured the pump−probe signals at $\omega_m = 2110$ cm⁻¹ ($v = 0\rightarrow1$) for the MgNCS⁺ CIP and at $\omega_m = 2032$ cm⁻¹ ($v = 1\rightarrow2$) for the free SCN⁻ ion. The pump−probe signals decay to a constant offset after 100 ps. This offset is about 2% of the amplitude of the pump−probe signal at $t = 0.1$ ps and results from the deposition of heat in the sample following vibrational population relaxation. When the vibrationally excited molecules relax to the ground state, their vibrational energy dissipates into the solvent bath leading to rapid local heating of the sample. We used a kinetic model developed initially for describing the vibrational population relaxation of liquid water to remove the heating contribution from the pump−probe signals.[45,69–71] These heating effects also occur in the 2DIR spectra at long time delays. The 2DIR spectrum at $T_w = 90$ ps shown in Figure 2 results from thermally induced changes in the vibrational

TABLE 2: Parameters Fitted to Orientational Anisotropy and Vibrational Lifetimes

	center freq (cm⁻¹)	b_1	τ_{or1} (ps)	b_2	τ_{or2} (ps)	T_1 (ps)
free SCN⁻ ($v = 1\rightarrow2$)	2032	0.09 ± 0.01	2.7 ± 0.5	0.25 ± 0.02	10.6 ± 0.6	10.7 ± 0.1
MgNCS⁺ ($v = 0\rightarrow1$)	2110	0.11 ± 0.02	5.7 ± 0.6	0.24 ± 0.02	85 ± 8	15.3 ± 0.1

Ligand Exchange Dynamics in Aqueous Solution

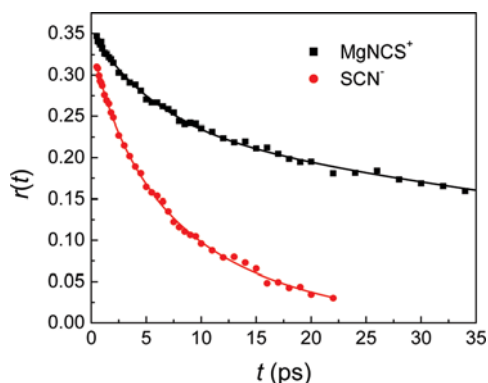*J. Phys. Chem. B, Vol. 114, No. 19, 2010* **6697**

Figure 4. Orientational anisotropy decay, $r(t)$. $r(t)$ for MgNCS$^+$ contact ion pair was measured at $\omega_{\mathrm{m}} = 2110$ cm^{-1} ($v = 0{\rightarrow}1$ transition). The $v = 1{\rightarrow}2$ transition of the CN stretching vibration of the MgNCS$^+$ contact ion pair overlaps with the $v = 0{\rightarrow}1$ transition of the CN stretching vibration of the free SCN$^-$ ion. Consequently, we probe $r(t)$ for the free SCN$^-$ ion at $\omega_{\mathrm{m}} = 2032$ cm^{-1} ($v = 1{\rightarrow}2$ transition). The biexponential fits to $r(t)$ are shown with solid lines.
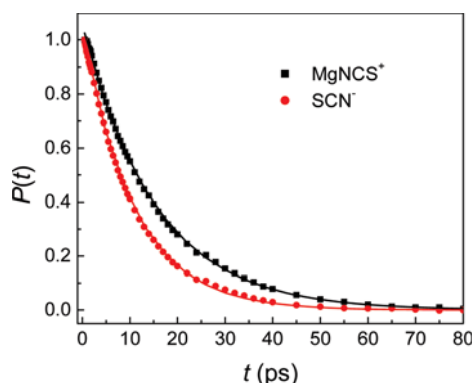

Figure 5. Vibrational population decays of the free SCN$^-$ ion and MgNCS$^+$ contact ion pair. Vibrational population decay for the free SCN$^-$ ion was measured at the $v = 1{\rightarrow}2$ transition (2032 cm^{-1}).

spectrum. We have carefully examined the impact of thermalization and determined it has a negligible effect on the 2DIR spectra for $T_{\mathrm{w}} \leq 40$ ps. The shift of the CIP $v = 0{\rightarrow}1$ absorption provides the most sensitive measure of thermalization, with the peak shifting to lower frequency with increasing temperature, and moves the dominant signal in the 2DIR spectrum off the diagonal. For $T_{\mathrm{w}} \leq 40$ ps, the signal remains on the diagonal, demonstrating the insignificant contribution of thermalization to the signal utilized to determine the chemical exchange dynamics.

We measured the IR pump−probe signals with the probe beam polarization parallel, $S_{\parallel}(t)$, and perpendicular, $S_{\perp}(t)$, to the pump beam polarization. These signals were used to obtain the vibrational population relaxation,

$$P(t) = S_{\parallel}(t) + 2S_{\perp}(t) \qquad (2)$$

and the orientational anisotropy,

$$r(t) = \frac{S_{\parallel}(t) - S_{\perp}(t)}{S_{\parallel}(t) + 2S_{\perp}(t)} = \frac{2}{5}C_{\mathrm{or}}(t) \qquad (3)$$

The orientational anisotropy, $r(t)$, measures the orientational relaxation dynamics of the CN stretch transition dipole as reflected by the second-order Legendre polynomial of the transition dipole correlation function, $C_2 = \langle P_2[\boldsymbol{\mu}(t) \cdot \boldsymbol{\mu}(0)] \rangle$,

while the population relaxation, $P(t)$, measures the decay of the vibrationally excited molecules. Figures 4 and 5 display $r(t)$ and $P(t)$ probed at 2110 cm^{-1} for the MgNCS$^+$ contact ion pair and 2032 cm^{-1} for the free SCN$^-$ ion, respectively. We fit the orientational anisotropy decay to a biexponential function,

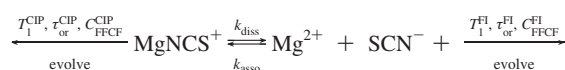$$r(t) = b_1 \exp(-t/\tau_{\mathrm{or1}}) + b_2 \exp(-t/\tau_{\mathrm{or2}}) \qquad (4)$$

The amplitude of the orientational anisotropy at $t = 0$ ps does not equal 0.4 because the measurement does not resolve the initial inertial rotation of the SCN$^-$ ions. The loss of orientational memory proceeds more slowly than the vibrational relaxation, so we do not observe the full anisotropic decay. We fit the normalized vibrational population relaxation to a single exponential function,

$$P(t) = A \exp(-t/T_1) \qquad (5)$$

Table 2 lists the parameters extracted from the fits to $r(t)$ and $P(t)$. It should also be noted that we measured a 20 ps lifetime for free SCN$^-$ in a 0.5 M aqueous SCN$^-$ solution, consistent with prior measurements.[40,72] The lifetime for the free SCN$^-$ ion decreases with increasing ionic concentration, leading to the much shorter lifetime reported in Table 3 than those measured previously.[40,72]

D. Numerical Calculation of 2DIR Spectra. We numerically calculated the linear IR spectrum and the T_{w}-dependent 2DIR spectra using the response function formalism based on diagrammatic perturbation theory with input parameters estimated from the linear and nonlinear experimental results.[73] Kwak et al. have described the response function formalism with two-species chemical exchange and the numerical calculation of 2DIR spectra in great detail,[74] which we outline here to facilitate the presentation of our results.

T_{w}-dependent 2DIR spectra of the free SCN$^-$ ions and the MgNCS$^+$ CIPs can be calculated for the ion association and dissociation dynamics by using the following scheme,

$$\underset{\text{evolve}}{\xleftarrow{T_1^{\mathrm{CIP}},\, \tau_{\mathrm{or}}^{\mathrm{CIP}},\, C_{\mathrm{FFCF}}^{\mathrm{CIP}}}} \mathrm{MgNCS}^+ \underset{k_{\mathrm{asso}}}{\overset{k_{\mathrm{diss}}}{\rightleftharpoons}} \mathrm{Mg}^{2+} + \mathrm{SCN}^- + \underset{\text{evolve}}{\xrightarrow{T_1^{\mathrm{FI}},\, \tau_{\mathrm{or}}^{\mathrm{FI}},\, C_{\mathrm{FFCF}}^{\mathrm{FI}}}}$$

where k_{asso} and k_{diss} are the association and dissociation rate constants, T_1^{FI} and T_1^{CIP} are the vibrational lifetimes, $\tau_{\mathrm{or}}^{\mathrm{FI}}$ and $\tau_{\mathrm{or}}^{\mathrm{CIP}}$ are the orientational relaxation times, and $C_{\mathrm{FFCF}}^{\mathrm{FI}}$ and $C_{\mathrm{FFCF}}^{\mathrm{CIP}}$ are the frequency−frequency correlation functions (FFCF) of free SCN$^-$ and the MgNCS$^+$ contact ion pair, respectively. Ignoring the activity coefficients of ionic species in solution, the equilibrium constant observed in spectroscopic measurements is given by

$$K_{\mathrm{eq}} = \frac{[\mathrm{Mg}^{2+}][\mathrm{SCN}^-]}{[\mathrm{MgNCS}^+]} = \frac{k_{\mathrm{diss}}}{k_{\mathrm{asso}}} \qquad (6)$$

where [···] represent the equilibrium concentrations. The concentrations [Mg^{2+}] and [SCN$^-$] correspond to a sum of the free ion, SIP, and 2SIP concentrations, though free ions will dominate as discussed previously.

Considering the concentration changes of free SCN$^-$ ions and MgNCS$^+$ CIP, the rate equations can be written as

$$\frac{d[\text{MgNCS}^+]}{dt} = -k_{\text{diss}}[\text{MgNCS}^+] + k_{\text{asso}}[\text{Mg}^{2+}][\text{SCN}^-]$$

$$\frac{d[\text{SCN}^-]}{dt} = k_{\text{diss}}[\text{MgNCS}^+] - k_{\text{asso}}[\text{Mg}^{2+}][\text{SCN}^-]$$

$$(7)$$

Since the solution contains an excess of $[\text{Mg}^{2+}]$, the concentration of $[\text{Mg}^{2+}]$ does not change significantly due to CIP formation. This allows the kinetics to be modeled as a pseudo-first-order reaction, with $k'_{\text{asso}} = k_{\text{asso}}[\text{Mg}^{2+}]$. These rate equations can be analytically solved with the boundary condition, $[\text{SCN}^-]$ $+[\text{MgNCS}^+] = $ constant, and the peak intensities in T_w-dependent 2DIR spectra are directly associated with the concentrations that are determined by the two-species exchange kinetics[43,45,75]

$$[\text{MgNCS}^+]_{\text{AA}}(T_\text{w}) = [\text{MgNCS}^+]\frac{k'_{\text{asso}} + k_{\text{diss}}\exp(-k_{\text{ex}}T_\text{w})}{k_{\text{ex}}}$$

$$[\text{SCN}^-]_{\text{BB}}(T_\text{w}) = [\text{SCN}^-]\frac{k_{\text{diss}} + k'_{\text{asso}}\exp(-k_{\text{ex}}T_\text{w})}{k_{\text{ex}}}$$

$$[\text{MgNCS}^+]_{\text{AB}}(T_\text{w}) = [\text{MgNCS}^+]\frac{k_{\text{diss}}(1 - \exp(-k_{\text{ex}}T_\text{w}))}{k_{\text{ex}}}$$

$$[\text{SCN}^-]_{\text{BA}}(T_\text{w}) = [\text{SCN}^-]\frac{k'_{\text{asso}}(1 - \exp(-k_{\text{ex}}T_\text{w}))}{k_{\text{ex}}}$$

$$(8)$$

where the exchange rate constant equals $k_{\text{ex}} = k_{\text{diss}} + k'_{\text{asso}}$, $[\text{MgNCS}^+]_{\text{AA}}(T_\text{w})$ and $[\text{SCN}^-]_{\text{BB}}(T_\text{w})$ are the concentrations associated with the diagonal peaks, and $[\text{MgNCS}^+]_{\text{AB}}(T_\text{w})$ and $[\text{SCN}^-]_{\text{BA}}(T_\text{w})$ are the concentrations associated with the cross peaks. The integrated intensity of the cross peaks in T_w-dependent 2DIR spectra depend on the exchange rate constant, k_{ex}.

The numerical calculation includes all of the dynamical features observed in the 2DIR spectra. As T_w increases, the amplitudes of peaks decay due to both vibrational population relaxation and orientational relaxation, while the peak shapes change from diagonally elongated to symmetrical as a result of spectral diffusion. In addition, the dissociation and association dynamics cause the cross peaks to grow in with increasing T_w. For the calculation of the linear and third-order nonlinear response functions for free SCN^- ion and MgNCS^+ ion pair in D_2O solution, it is assumed that the bath fluctuations of free SCN^- ion and MgNCS^+ contact ion pair in D_2O solution follow Gaussian statistics (second-order cumulant approximation) and the transition dipole moment of the CN stretch does not depend on the nuclear coordinates (Condon approximation). We use the harmonic approximation to scale the transition dipole moments, $\mu_{01}/\mu_{12} = 2^{1/2}$, and the IR pulses are assumed to be impulsive.

We estimate the vibrational lifetimes (T_1) and orientational relaxation times (τ_{or}) of the free SCN^- anions and the MgNCS^+ CIP with the values extracted from the polarization-selective IR pump−probe experiments and use them as initial input parameters for the response function calculations. They only provide estimates because the pump−probe measurements integrate the response of all molecules with the same transition frequency when the probe pulse arrives at the sample, independent of their prior chemical history. The extent to which the true parameters differ from the pump−probe parameters depends upon the relative intensity of the diagonal and cross-peak intensities and the magnitude of the difference in the orientational and population dynamics of the exchanging chemical species. The dominance of the diagonal peaks in the 2DIR spectra indicates that the pump−probe measurements should provide excellent estimates for the vibrational lifetimes and orientational relaxation times, a conclusion supported by the numerical simulations. The FFCFs for the free SCN^- anion and the MgNCS^+ CIP are modeled by

$$C_{\text{FFCF}}(t) = \frac{\delta(t)}{T_2} + \Delta_1^2\exp(-t/\tau_1) + \Delta_2^2\exp(-t/\tau_2)$$

$$(9)$$

The first term represents the homogeneous broadening component, which is motionally narrowed. The two Kubo terms are used to describe the inhomogeneous broadening components. Under the short time approximation, the normalized FFCF is directly proportional to the $C_{\text{CLS}}(T_\text{w})$.[59,62] The $C_{\text{CLS}}(T_\text{w})$ are fit with a biexponential function (eq 1) as shown in Table 1. From the amplitudes, a_1 and a_2, of the biexponential fit, Δ_1 and Δ_2 are obtained by $\Delta_i \cong a_i^{1/2}\Gamma_{\text{fwhm}}/(2[2\ln(2)]^{1/2})$, where Γ_{fwhm} is the peak width in the FTIR spectrum.[59] The $C_{\text{FFCF}}(t)$ can be fully obtained when the homogeneous broadening component, $\Gamma = 1/(\pi T_2)$, is determined.

We iteratively fit all other parameters in the response function formalism by minimizing the difference between the numerically calculated linear IR absorption spectrum and T_w-dependent 2DIR spectra and the experimental results. The iterative fit varied the ratios of transition dipole moments $\mu_{01}(\text{MgNCS}^+)/\mu_{01}(\text{SCN}^-)$, the concentration ratio, $[\text{MgNCS}^+]/[\text{SCN}^-]$, the dissociation rate constant, k_{diss}, and the values of T_2 in eq 9 for both free SCN^- ion and MgNCS^+ CIP. Figure 6B displays the 2DIR spectra calculated with the response function formalism with the best fit parameters summarized in Table 3. Most significantly, we extract the dissociation and association time constants, $\tau_{\text{diss}} = 1/k_{\text{diss}} = 52 \pm 10$ ps and $\tau_{\text{asso}} = 1/k'_{\text{asso}} = 1/(K_{\text{eq}}k_{\text{diss}}) = 140 \pm 30$ ps. The calculated 2DIR spectra with $\tau_{\text{diss}} = \infty$ also appear in Figure 6C for comparison.

IV. Discussion

A. Kinetics of Ion Exchange. The 2DIR measurement observes the association of Mg^{2+} and SCN^- to form a contact ion pair with a time constant of $\tau_{\text{asso}} = 1/k'_{\text{asso}} = 140 \pm 30$ ps. This time constant results from the replacement of water and perchlorate ligands within the first solvation shell of the Mg^{2+} cation. The picosecond time scale observed in the experiment does not conform with ultrasonic relaxation measurements or

TABLE 3: Parameters Used for Numerical Calculation of Linear IR Spectrum and T_w-Dependent 2DIR Spectra

	T_1 (ps)	τ_{or} (ps)	Γ (cm^{-1})	Δ_1 (cm^{-1})	τ_1 (ps)	Δ_2 (cm^{-1})	τ_2 (ps)	μ_{01}	concn
free SCN$^-$	10.7	8.4	11.3	10.8	1.11	11.8	8.25	0.97	2.66
MgNCS+	15.3	42.5	9.25	8.28	1.64	6.57	9.95	1	1

*The numerical calculation use single exponential decays for the population and the orientational relaxation. The values listed for T_1 and τ_{or} correspond to the best fits of the experimental data to single exponential decays.

Ligand Exchange Dynamics in Aqueous Solution

J. Phys. Chem. B, Vol. 114, No. 19, 2010 **6699**

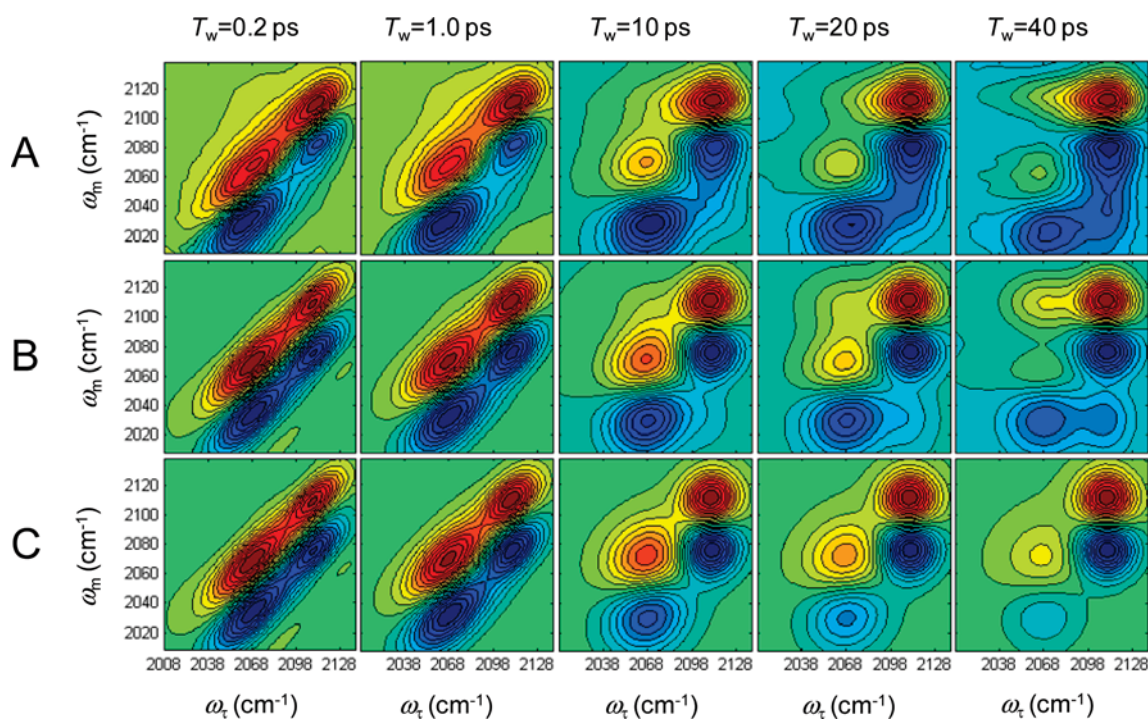**Figure 6.** Comparison of experimental and calculated 2DIR spectra. (A) Experimental 2DIR spectra of $Mg(ClO_4)_2$ and NaSCN dissolved in D_2O. The high-frequency peak at $\omega_\tau = \omega_m = 2110$ cm^{-1} corresponds to the MgNCS$^+$ ion pair with an anharmonicity of 28 cm^{-1}. The low-frequency peak at $\omega_\tau = \omega_m = 2068$ cm^{-1} corresponds to the free SCN$^-$ ion with an anharmonicity of 40 cm^{-1}. (B) Calculated 2DIR spectra with a response function formalism that includes two-species exchange kinetics with a dissociation time of $\tau_{diss} = 52$ ps. (C) Calculated 2DIR spectra with a dissociation time of $\tau_{diss} = \infty$. Clearly, ion association and dissociation dynamics must be included to accurately reproduce the experimental 2DIR spectra.

the standard interpretation of the Eigen−Tamm model, where diffusion controls the doubly solvent separated ion pair kinetics and thermal activation controls contact ion pair kinetics.[23,34,47,49] The microsecond time scale for CIP formation observed in ultrasonic relaxation measurements of aqueous MgSO$_4$ solutions[23,34,47,49] has been correlated with the water exchange rate around the cation.[51] While these frequency domain observations have not been replicated with time domain measurements, the 7.4 kcal/mol activation energy extracted from first-principles MD simulations[16] resembles the 9.5 kcal/mol activation energy measured with NMR.[50] Unless the presence of SCN$^-$ and ClO$_4^-$ ligands greatly modifies the binding energy of water to Mg^{2+},[12,15] the exchange process being observed experimentally seems unlikely to be the interchange of water and SCN$^-$ in the first solvation shell of Mg^{2+}. For these reasons, we conclude that the time constant for CIP dissociation extracted from our experiments likely results from a different dynamical process. We attribute the observed dynamics to anion ligand exchange around the Mg^{2+} ion. While perchlorate and thiocyanate anions coordinate more weakly than water with magnesium cations, the very high ionic concentration used in our measurements leads to a significant number of perchlorate anions in the first solvation shell of Mg^{2+} ion, as confirmed by Raman measurements.[36] Since MgNCS$^+$ and MgClO$_4^+$ associate much more weakly than Mg^{2+}−H$_2$O, the dissociation rate of anion ligands from Mg^{2+} ion would be expected to be much faster, as seen in our measurement.

B. Orientational Relaxation Dynamics of Free SCN$^-$ Ion and MgNCS$^+$ Ion Pair. The orientational anisotropy decay of the free SCN$^-$ ion and MgNCS$^+$ contact ion pair in D$_2$O appear in Figure 4. The orientational anisotropy of the free SCN$^-$ ion decays much faster than that of the MgNCS$^+$ CIP. Both orientational anisotropies exhibit biexponential decays, with time constants of 2.7 ± 0.5 and 10.6 ± 0.6 ps for the free SCN$^-$ ion

and 5.7 ± 0.6 and 85 ± 8 ps for the MgNCS$^+$ CIP. The appearance of biexponential dynamics clearly demonstrates a strong deviation from the simple hydrodynamics expected for a symmetric top with the transition dipole parallel to the high symmetry axis.[76,77] The validity of a continuum description of microscopic dynamics improves greatly when the solute being interrogated experimentally has a size much larger than the solvent. Given that the SCN$^-$ solute has a size comparable to the solvent D$_2$O, a strong deviation from hydrodynamics should be expected. The factor of 8 slower dynamics of the CIP further demonstrates the deviation from visco-elastic behavior. For the Stokes−Einstein−Debye equation, the rotational time constant should be proportional to the solute volume. Given the ionic radii of 2.2 Å for SCN$^-$ [78] and 0.8 Å for Mg^{2+},[79] the rotational times should differ by roughly a factor of 2.5, rather than a factor of 8.

Biexponential orientational relaxation can be interpreted with the restricted orientational diffusion model of Lipari and Szabo.[80,81] Within this model, fast orientational diffusion with diffusion constant, D_c, can occur within a restricted cone of semiangle θ_c, after which the cone orientationally diffuses on the surface of the full sphere with a second diffusion constant, D_θ.[82] While the exact expression for $C_2(t)$ in the restricted orientational diffusion model involves an infinite sum of exponentials,[80−82] an accurate approximation can be made for cone semiangles $\theta_c < 60°$. The approximate model gives

$$C_2(t) = S^2 \exp(-6D_\theta t) + [1 - S^2] \exp(-t[1/\tau_{eff} + 6D_\theta]) \tag{10}$$

Within this model, $1 - S^2$ represents the fraction of the anisotropy that decays due to orientational diffusion within the restricted cone, τ_{eff} represents the characteristic time for orien-

tational diffusion within the cone, and D_θ represents the orientational diffusion constant for diffusion outside of the cone. The cone semiangle can be determined from $S^2 = \langle P_2(\cos\theta_c)\rangle^2$, where $P_2(x) = (3x^2 - 1)/2$. The slow component of the CIP orientational relaxation equals 0.24 ± 0.02 of $r(t)$, or 0.6 of $C_2(t)$, and $\theta_c = 23(\pm 1)°$. The cone semiangle reflects the angular degree of freedom of the SCN$^-$ ion within the CIP, where full orientation relaxation requires the orientational motion of the intact ion pair. The restricted orientational motion could originate from a strong interaction between the charge on the Mg^{2+} and the dipole on the SCN$^-$, since the charge−charge interaction will not restrict SCN$^-$ rotation about its center of mass.

The restricted orientational diffusion model also allows the orientational diffusion constant for orientational relaxation within the cone, D_c, to be determined from D_θ and τ_{eff}. First, we use τ_{or1} and τ_{or2} to determine τ_{eff} and D_θ: $D_\theta^{-1} = 6\tau_{or2} = 510$ ps and $\tau_{eff} = [1/\tau_{or1} - 6D_\theta]^{-1} = 6.1$ ps. Lipari and Szabo provide an approximate solution for D_c from τ_{eff} and θ_c when $\theta_c < 60°$,

$$D_c\tau_{eff}(1 - S^2) = -x_0^2(1 + x_0)^2\{\ln[(1 + x_0)/2] + (1 - x_0)/2\}/$$
$$[2(1 - x_0)] + (1 - x_0)(6 + 8x_0 - x_0^2 - 12x_0^3 - 7x_0^4)/24 \quad (11)$$

where $x_0 = \cos\theta_c$. Using the values listed above, we get $D_c^{-1} = 250 \pm 30$ ps, roughly a factor of 2 faster than D_θ^{-1}.

Application of similar analysis to the biexponential behavior of the 'free' SCN$^-$ ion gives $\theta_c = 22 \pm 1°$, $D_\theta^{-1} = 6\tau_{or2} = 64$ ps, and $D_c^{-1} = 160 \pm 20$ ps. Since the 2068 cm^{-1} peak has small contributions from doubly solvent separated ions and solvent separated ions, as well as the "free" SCN$^-$ ion, these orientational dynamics do not represent free anion dynamics solely.

Before closing, we would like to comment on the orientational relaxation time and dissociation time of the MgNCS$^+$ contact ion pair. We have determined the rate of the slow component of the orientational relaxation to be smaller than the CIP dissociation rate. This merely indicates that a CIP likely dissociates before all orientational memory has been lost, not an unphysical conclusion. Additionally, such a comparison does not address the difference in the functional form for the anisotropy, biexponential, and the exchange, single exponential. Using a $1/e$ time, $\tau_{1/e}$, for both, we find this mean rotational time of 42 ps to be faster than the dissociation rate. We believe this reflects the fact that the orientational relaxation and MgNCS$^+$ contact ion pair dissociation occur on a similar time scale.

C. Spectral Diffusion Dynamics of Free SCN$^-$ Ion and MgNCS$^+$ Ion Pair. The combination of the FTIR absorption spectrum and peak shape analysis of the T_w-dependent 2DIR spectra provide a detailed measure of the frequency−frequency correlation function (FFCF) of the SCN$^-$ ion in both free anion and CIP configurations.[59−63] The FFCF characterizes how fluctuations in the SCN$^-$ chromophore environment influence the solute stability. Our measurement allows us to characterize how the ion configurations influence the solvation dynamics. This represents a measurement of potential importance because prior theoretical studies have indicated that the symmetry of the charge distribution on the solute has a significant impact on resultant solvation dynamics but this prediction has not been thoroughly investigated experimentally.[83,84]

As discussed in Section III.B, we use the center line slope (CLS) method to quantify the FFCFs from the T_w-dependent 2DIR spectra. The inverse of the CLS provides a partial measure of the normalized FFCFs for the free anion and the contact ion

pair. The CLS method cannot measure the spectral diffusion dynamics of any component of the FFCF that is motionally narrowed. Consequently, the plots in Figure 3 do not extrapolate to unity at time zero. The component missing from the FFCF results from the homogeneously broadened component, which is given by $\Gamma = 1/(\pi T_2)$. Recently, it has been shown that the full FFCF with the homogeneous broadening component can be determined by simple fits to the $C_{CLS}(T_w)$ and the linear FTIR spectrum.[61] By including the homogeneous broadening component, the full FFCFs of SCN$^-$ ions are modeled by eq 9. The inhomogeneous line width of an absorption peak is described by two Kubo terms, while the homogeneous line width is given by $\Gamma = 1/\pi T_2$, where $1/T_2 = (1/T_2^*) + (1/2T_1) + (1/3T_{or})$. Here, T_2^*, T_1, and T_{or} represent the pure dephasing time, lifetime, and orientational relaxation time, respectively. The parameters for the FFCFs of SCN$^-$ ions in the free anion and CIP configuration are summarized in Table 3.

Given the significant difference in the charge distribution of the free anion and the CIP, the solvation of each anion configuration need not be similar. This difference does manifest in the inhomogeneous widths of the vibrational peaks, with the free anion inhomogenous width being 50% wider than the inhomogenous width for the CIP, but not in the solvation dynamics. Our result does appear consistent with prior studies that indicate that the solvent determines the spectral diffusion dynamics, with little anion-dependent variation.[57] The similar rates of spectral diffusion contrast with the orientational relaxation rates, where, as opposed to the free SCN$^-$ ion, the CIP exhibits a significantly slower rate of rotation that cannot be fully accounted for with the difference in their molecular volume.

V. Closing Remarks

We have utilized ultrafast IR spectroscopy to study the conformational and structural dynamics of an aqueous ionic solution. We have used 2DIR spectroscopy of the CN stretching vibration of the SCN$^-$ ion to measure the chemical exchange dynamics between free SCN$^-$ ions and MgNCS$^+$ contact ion pairs (CIP) in a solution of NaSCN and Mg(ClO$_4$)$_2$ dissolved in D$_2$O. The CN stretch of the SCN$^-$ anion provides a sensitive spectroscopic probe of the ion configuration, with the CIP absorption blue-shifted from the free ion absorption. We have also used 2DIR spectroscopy and polarization-dependent IR pump−probe spectroscopy to measure the spectral diffusion and orientational relaxation dynamics of the free SCN$^-$ anion and the CIP.

The 2DIR experiments have determined the dissociation time constant for the MgNCS$^+$ contact ion pair to be 52 ± 10 ps in D$_2$O. This dissociation results from the replacement of SCN$^-$ ions by perchlorate ions within the first solvation shell of the Mg^{2+} cation. Water ligand exchange from the Mg^{2+} first solvation shell has been measured to take microseconds with multiple prior measurements,[34,47,49,50] so we attribute the observed picosecond process to perchlorate−thiocyanate anion exchange in the first solvation shell of Mg^{2+}. While perchlorate and thiocyanate anions coordinate more weakly than water with magnesium cations, the very high ionic concentration used in our measurements leads to a significant number of perchlorate anions in the first solvation shell of Mg^{2+}, as confirmed by Raman measurements.[36] The weaker association of MgNCS$^+$ and MgClO$_4^+$ CIPs leads to the faster rate of exchange observed experimentally. We intend to investigate the ligand exchange mechanism by replacing perchlorate with alternative anions. Varying the strength of the Mg^{2+}−anion interaction should

Ligand Exchange Dynamics in Aqueous Solution

J. Phys. Chem. B, Vol. 114, No. 19, 2010 **6701**

modify the ligand exchange rate and provide further evidence for the ligand exchange mechanism we have proposed.

The biexponential orientational dynamics of the free SCN^- anion and the SCN^- anion in the CIP differ significantly. The significantly slower rotational dynamics of the anion in the CIP demonstrate that the anion does not freely rotate in the CIP, most likely due to the Mg^{2+}-charge SCN^-–dipole interaction. The orientational relaxation dynamics also deviate from simple hydrodynamic behavior, as exemplified by the biexponential orientational dynamics and the deviation of the ratio of the slower rotational time constants, $\tau_{or2}^{Fl}/\tau_{or2}^{CIP}$, from the ratio of the ionic volumes, V^{Fl}/V^{CIP}. The spectral diffusion dynamics also occur on two time scales for both anion configurations. While the spectral diffusion also occurs more slowly for SCN^- in the CIP, the rate does not differ much from that seen for the free SCN^-.

The variation in the orientational relaxation and spectral diffusion dynamics observed for the free anion and the anion in the contact ion pair reflect the distinct manner with which the solvent solvates this different charge distribution and determines the rate with which these distinct charge configurations interconvert. While the measurements alone cannot determine the mechanism for ligand exchange and ion solvation, these measurements do provide a dynamical benchmark for comparison with molecular dynamics simulations that complements the traditional thermodynamic and structural benchmarks.[14,15,17]

Supporting Information Available: FTIR spectra of alkali metal thiocyanate salts. This material is available free of charge via the Internet at http://pubs.acs.org.

References and Notes

(1) Woutersen, S.; Mu, Y.; Stock, G.; Hamm, P. *Chem. Phys.* **2001**, *266*, 137.

(2) Zheng, J.; Kwak, K.; Asbury, J. B.; Chen, X.; Piletic, I.; Fayer, M. D. *Science* **2005**, *309*, 1338.

(3) Kim, Y. S.; Hochstrasser, R. M. *Proc. Natl. Acad. Sci. U.S.A.* **2005**, *102*, 11185.

(4) Zheng, J.; Kwak, K.; Xie, J.; Fayer, M. D. *Science* **2006**, *313*, 1951.

(5) Rey, R.; Guardia, E. *J. Phys. Chem.* **1992**, *96*, 4712.

(6) Smith, D. E.; Dang, L. X. *J. Chem. Phys.* **1994**, *100*, 3757.

(7) Geissler, P. L.; Dellago, C.; Chandler, D. *J. Phys. Chem. B* **1999**, *103*, 3706.

(8) Chen, A. A.; Pappu, R. V. *J. Phys. Chem. B* **2007**, *111*, 6469.

(9) Kim, H. J.; Hynes, J. T. *J. Am. Chem. Soc.* **1992**, *114*, 10508.

(10) Rey, R.; Guàrdia, E.; Padró, J. A. *J. Chem. Phys.* **1992**, *97*, 1343.

(11) Pasquarello, A.; Petri, I.; Salmon, P. S.; Parisel, O.; Car, R.; Tóth, É.; Powell, D. H.; Fischer, H. E.; Helm, L.; Merbach, A. *Science* **2001**, *291*, 856.

(12) Tongraar, A.; Sagarik, K.; Rode, B. M. *J. Phys. Chem. B* **2001**, *105*, 10559.

(13) Lightstone, F. C.; Schwegler, E.; Hood, R. Q.; Gygi, F.; Galli, G. *Chem. Phys. Lett.* **2001**, *343*, 549.

(14) Rode, B. M.; Schwenka, C. F.; Tongraarb, A. *J. Mol. Liq.* **2004**, *110*, 105.

(15) Rode, B. M.; Schwenk, C. F.; Hofer, T. S.; Randolf, B. R. *Coord. Chem. Rev.* **2005**, *249*, 2993.

(16) Ikeda, T.; Boero, M.; Terakura, K. *J. Chem. Phys.* **2007**, *127*, 074510.

(17) Fennell, C. J.; Bizjak, A.; Vlachy, V.; Dill, K. A. *J. Phys. Chem. B* **2009**, *113*, 6782.

(18) Eigen, M. *Discuss. Faraday Soc.* **1954**, *17*, 194.

(19) Eigen, M.; Eyring, E. M. *J. Am. Chem. Soc.* **1962**, *84*, 3254.

(20) Davies, C. W. *Ion Association*; Butterworths: London, UK, 1962.

(21) Barthel, J.; Buchner, R.; Eberspächer, P.-N.; Münsterer, M.; Stauber, J.; Wurm, B. *J. Mol. Liq.* **1998**, 83.

(22) Bešter-Rogač, M.; Neueder, R.; Barthel, J. *J. Solution Chem.* **2000**, *29*, 51.

(23) Kaatze, U.; Hushcha, T. O.; Eggers, F. *J. Solution Chem.* **2000**, *29*, 299.

(24) Barthel, J.; Buchner, R.; Wismeth, E. *J. Solution Chem.* **2000**, *29*, 937.

(25) Fratiello, A.; Kubo-Anderson, V.; Lee, R. A.; Patrick, M.; Perrigan, R. D.; Porras, T. R.; Sharp, A. K.; Wong, K. *J. Solution Chem.* **2001**, *30*, 77.

(26) Rudolph, W. W.; Mason, R. *J. Solution Chem.* **2001**, *30*, 527–548.

(27) Bešter-Rogač, M.; Tomšič, M.; Barthel, J.; Neueder, R.; Apelblat, A. *J. Solution Chem.* **2002**, *31*, 1.

(28) Tomšič, M.; Bešter-Rogač, M.; Jamnik, A.; Neueder, R.; Barthel, J. *J. Solution Chem.* **2002**, *31*, 19.

(29) Buchner, R.; Samani, F.; May, P. M.; Sturm, P.; Hefter, G. *ChemPhysChem.* **2003**, *4*, 373.

(30) Akilan, C.; Rohman, N.; Hefter, G.; Buchner, R. *ChemPhysChem.* **2006**, *7*, 2319.

(31) Wachter, W.; Fernandez, S.; Buchner, R.; Hefter, G. *J. Phys. Chem. B* **2007**, *111*, 9010.

(32) Owrutsky, J. C.; Pomfret, M. B.; Barton, D. J.; Kidwell, D. A. *J. Chem. Phys.* **2008**, *129*, 024513.

(33) Buchner, R.; Chen, T.; Hefter, G. *J. Phys. Chem. B* **2004**, *108*, 2365.

(34) Atkinson, G.; Petrucci, S. *J. Phys. Chem.* **1966**, *70*, 3122.

(35) Marcus, Y. *Ion Solvation*; Wiley: New York, 1985.

(36) Antic-Jovanovic, A.; Jeremic, M.; Lalic, M. *J. Raman Spectrosc.* **1989**, *20*, 523.

(37) Krestov, G. A.; Novosyolov, N. P.; Perelygin, I. S. *Ionic Solvation*; Wiley, New York, 1994.

(38) Le Borgne, C.; Illien, B.; Beignon, M.; Chabanel, M. *Phys. Chem. Chem. Phys.* **1999**, *1*, 4701.

(39) Zhong, Q.; Owrutsky, J. C. *Chem. Phys. Lett.* **2004**, *383*, 176.

(40) Lenchenkov, V.; She, C.; Lian, T *J. Phys. Chem. B* **2006**, *110*, 19990.

(41) Ohta, K.; Tominaga, K. *Chem. Phys. Lett.* **2006**, *429*, 136.

(42) Fayer, M. D. *Annu. Rev. Phys. Chem.* **2008**, *60*, 21.

(43) Cho, M. *Two-Dimensional Optical Spectroscopy*; CRC Press: Boca Raton, FL, 2009.

(44) Ishikawa, H.; Kwak, K.; Chung, J. K.; Kim, S.; Fayer, M. D. *Proc. Nat. Acad. Sci. U.S.A.* **2008**, *105*, 8619.

(45) Park, S.; Odelius, M.; Gaffney, K. J *J. Phys. Chem. B* **2009**, *113*, 7825.

(46) Moilanen, D. E.; Wong, D.; Rosenfeld, D. E.; Fenn, E. E.; Fayer, M. D. *Proc. Natl. Acad. Sci. U.S.A.* **2009**, *106*, 375.

(47) Eigen, M.; Tamm, K. *Z. Elektrochem.* **1962**, *66*, 107.

(48) Neely, J.; Connick, R. *J. Am. Chem. Soc.* **1970**, *92*, 3476.

(49) Evans, D. F.; Matesich, S. M. A. *J. Solution Chem.* **1973**, *2*, 193.

(50) Bleuzen, A.; Pittet, P.-A.; Helm, L.; Merbach, A. E. *Magn. Reson. Chem.* **1997**, *35*, 765.

(51) Marcus, Y.; Hefter, G. *Chem. Rev.* **2006**, *106*, 4585.

(52) Laenen, R.; Rausch, C.; Laubereau, A. *Phys. Rev. Lett.* **1998**, *80*, 2622.

(53) Gale, G. M.; Gallot, G.; Hache, F.; Lascoux, N.; Bratos, S.; Leicknam, J. C. *Phys. Rev. Lett.* **1999**, *82*, 1068.

(54) Piletic, I. R.; Gaffney, K. J.; Fayer, M. D. *J. Chem. Phys.* **2003**, *119*, 423.

(55) Hamm, P.; Lim, M.; Hochstrasser, R. M. *Phys. Rev. Lett.* **1998**, *81*, 5326.

(56) Fecko, C. J.; Eaves, J. D.; Loparo, J. J.; Tokmakoff, A.; Geissler, P. L. *Science* **2003**, *301*, 1698.

(57) Ohta, K.; Tominaga, K. *Bull. Chem. Soc. Jpn.* **2005**, *78*, 1581.

(58) Demirdoven, N.; Khalil, M.; Tokmakoff, A. *Phys. Rev. Lett.* **2002**, *89*, 237401.

(59) Kwak, K.; Park, S.; Finkelstein, I. J.; Fayer, M. D. *J. Chem. Phys.* **2007**, *127*, 1245031.

(60) Park, S.; Fayer, M. D. *Proc. Nat. Acad. Sci. U.S.A.* **2007**, *104*, 16731.

(61) Park, S.; Moilanen, D. E.; Fayer, M. D. *J. Phys. Chem. B* **2008**, *102*, 5279.

(62) Kwak, K.; Rosenfeld, D. E.; Fayer, M. D. *J. Chem. Phys.* **2008**, *128*, 204505.

(63) Park, S.; Kwak, K.; Fayer, M. D. *Laser Phys. Lett.* **2007**, *4*, 704.

(64) Zheng, J.; Kwak, K.; Fayer, M. D. *Acc. Chem. Res.* **2007**, *40*, 75.

(65) Khalil, M.; Demirdoven, N.; Tokmakoff, A. *Phys. Rev. Lett.* **2003**, *90* (4), 047401.

(66) Moilanen, D. E.; Piletic, I. R.; Fayer, M. D. *J. Phys. Chem. C* **2007**, *111*, 8884.

(67) Park, S.; Gaffney, K. J. Unpublished results.

(68) Cahoon, J. F.; Sawyer, K. R.; Schlegel, J. P.; Harris, C. B. *Science* **2008**, *319*, 1820.

(69) Steinel, T.; Asbury, J. B.; Zheng, J. R.; Fayer, M. D. *J. Phys. Chem. A* **2004**, *108*, 10957.

(70) Dokter, A. M.; Woutersen, S.; Bakker, H. J. *Phys. Rev. Lett.* **2005**, *94*, 178301.

(71) Piletic, I.; Moilanen, D. E.; Spry, D. B.; Levinger, N. E.; Fayer, M. D. *J. Phys. Chem. A* **2006**, *110*, 4985.

(72) Li, M.; Owrutsky, J.; Sarisky, M.; Culver, J. P.; Yodh, A.; Hochstrasser, R. M. *J. Chem. Phys.* **1993**, *98*, 5499.

(73) Mukamel, S. *Principles of Nonlinear Optical Spectroscopy*; Oxford University Press: New York, 1995.

(74) Kwak, K.; Zheng, J.; Cang, H.; Fayer, M. D. *J. Phys. Chem. B* **2006**, *110*, 19998.

(75) Kwac, K.; Cho, M. *J. Chem. Phys.* **2004**, *120*, 1477.

(76) Chuang, T. J.; Eisenthal, K. B. *J. Chem. Phys.* **1972**, *57*, 5094.

(77) Berne, B. J.; Pecora, R. *Dynamic Light Scattering*; J. Wiley: New York, 1976.

(78) Iwadate, Y.; Kawamura, K.; Igarashi, K.; Mochinaga, J. *J. Phys. Chem.* **1982**, *86*, 5205.

(79) *CRC Handbook of Chemistry and Physics*, 90th ed.; Taylor and Francis Group LLC: Boca Raton, FL, 2010.

(80) Lipari, G.; Szabo, A *Biophys. J.* **1980**, *30*, 489.

(81) Lipari, G.; Szabo, A. *J. Am. Chem. Soc.* **1982**, *104*, 4546.

(82) Gaffney, K. J.; Piletic, I. R.; Fayer, M. D. *J. Chem. Phys.* **2003**, *118*, 2270.

(83) Raineri, F. O.; Resat, H.; Perng, B.-C.; Hirata, F.; Friedman, H. L. *J. Chem. Phys.* **1994**, *100*, 1477.

(84) Ladanyi, B. M.; Stratt, R. M. *J. Phys. Chem.* **1996**, *100*, 1266.